REPORT DOCUMENTATION PAGE	*Form Approved OMB No. 0704-0188*

1. REPORT DATE *(DD-MM-YYYY)*	2. REPORT TYPE	3. DATES COVERED *(From - To)*
SEP 06	Conference Paper Postprint	Oct 04 - Apr 06

4. TITLE AND SUBTITLE	
INJECTION CHARACTERIZATION OF PACKAGED BI-DIRECTIONAL DIAMOND SHAPED RING LASERS AT 1550 NM	5a. CONTRACT NUMBER IN-HOUSE
	5b. GRANT NUMBER N/A
	5c. PROGRAM ELEMENT NUMBER 62204F
6. AUTHOR(S) Rebecca Bussjager, Reinhard Erdmann, Vassillios Kovanis, Brian McKeon, Michael Fanto, Steve Johns, Michael Hayduk, Joseph Osman , Alan Morrow, Malcolm Green, Nancy Stoffel, Songsheng Tan, Charles Shick, Wesley Bacon, Bryan Beaman,	5d. PROJECT NUMBER SEMI
	5e. TASK NUMBER SN
	5f. WORK UNIT NUMBER 01

7. PERFORMING ORGANIZATION NAME(S) AND ADDRESS(ES)	8. PERFORMING ORGANIZATION REPORT NUMBER
AFRL/SNDP 25 Electronic Pky Rome NY 13441-4515	AFRL-SN-RS-TP-2006-15
9. SPONSORING/MONITORING AGENCY NAME(S) AND ADDRESS(ES)	**10. SPONSOR/MONITOR'S ACRONYM(S)**
AFRL/SNDP 25 Electronic Pky Rome NY 13441-4515	
	11. SPONSOR/MONITOR'S REPORT NUMBER(S) AFRL-SN-RS-TP-2006-15

12. DISTRIBUTION/AVAILABILITY STATEMENT

Approved for public release; distribution unlimited. SN-06-0153 / AFRL/WS-06-0993

13. SUPPLEMENTARY NOTES

©2006 SPIE. This work has been published in the Proceedings for SPIE AeroSense Conference., 2006. The US Government has for itself and others acting on its behalf an unlimited, paid-up, nonexclusive, irrevocable worldwide license to use, modify, reproduce,

14. ABSTRACT

The Air Force Research Laboratory, Binoptics Corp., and Infotonics Technology Center worked collaboratively to package and characterize recently developed diode based ring lasers that operate at 1550 nm in a diamond shaped cavity. The laser modes propagate bi-directionally; however, uniaxial propagation may be induced by optical injection or by integrating a mirror. Round trip cavity length was 500 µm in 3.5 µm wide ridge waveguides, and four polarization maintaining lensed fibers provided access to the input and output modes. A signal from a tunable diode laser, incident at one port, served to injection lock both of the counter-propagating circulating modes. When the input signal was timeencoded by an optical modulator, the encoding was transferred to both modes with an inverted time-intensity profile. Performance, in terms of fidelity and extinction ratio, is characterized for selected pulsed and monochromatic formats from low frequencies to those exceeding 12 GHz. A rate equation model is proposed to account for certain aspects of the observed behavior and analog and digital applications are discussed.

15. SUBJECT TERMS

bi-directional semiconductor ring lasers, diamond shaped, laser injection

16. SECURITY CLASSIFICATION OF: a. REPORT	b. ABSTRACT	c. THIS PAGE	17. LIMITATION OF ABSTRACT	18. NUMBER OF PAGES	19a. NAME OF RESPONSIBLE PERSON
					Rebecca J. Bussjager, Program Manager
U	U	U	UL	13	19b. TELEPHONE NUMBER *(Include area code)* 315-330-2918

Injection characterization of packaged bi-directional diamond shaped ring lasers at 1550 nm

Rebecca Bussjager[a], Reinhard Erdmann[a], Vassillios Kovanis[a], Brian McKeon[a], Michael Fanto[a], Steve Johns[a], Michael Hayduk[a], Joseph Osman[a], Alan Morrow[b], Malcolm Green[b], Nancy Stoffel[c], Songsheng Tan[c], Charles Shick[c], Wesley Bacon[d], Bryan Beaman[d]

[a]Air Force Research Laboratory/SNDP, 25 Electronic Pkwy, Rome, NY 13441
[b]Binoptics Corporation, 9 Brown Road, Ithaca, NY 14850
[c]Infotonics Technology Center, 5450 Campus Drive, Canandaigua, NY 14424
[d]Kodak Research Laboratory, 1999 Lake Avenue, Rochester, NY 14650

ABSTRACT

The Air Force Research Laboratory, Binoptics Corp., and Infotonics Technology Center worked collaboratively to package and characterize recently developed diode based ring lasers that operate at 1550 nm in a diamond shaped cavity. The laser modes propagate bi-directionally; however, uniaxial propagation may be induced by optical injection or by integrating a mirror. Round trip cavity length was 500 µm in 3.5 µm wide ridge waveguides, and four polarization-maintaining lensed fibers provided access to the input and output modes. A signal from a tunable diode laser, incident at one port, served to injection lock both of the counter-propagating circulating modes. When the input signal was time-encoded by an optical modulator, the encoding was transferred to both modes with an inverted time-intensity profile. Performance, in terms of fidelity and extinction ratio, is characterized for selected pulsed and monochromatic formats from low frequencies to those exceeding 12 GHz. A rate equation model is proposed to account for certain aspects of the observed behavior and analog and digital applications are discussed.

KEYWORDS: bi-directional semiconductor ring lasers, diamond shaped, laser injection

1. INTRODUCTION

Binoptics Corporation has demonstrated a new diamond shaped cavity configuration for semiconductor (SC) ring lasers that operate in the low loss fiber window near 1550 nm. Their novel etched facet technology allows facets to be defined through high precision photolithography, rather than traditional cleaving, offering flexibility and reproducibility in monolithic integration capability[1]. The laser modes propagate bi-directionally, but the extent of uniaxial propagation can be influenced by laser injection[2] at the ring's resonance or by implementing a mirror external to the cavity to suppress one of the modes. The induced intensity inversion of the mode counter-propagating relative to the input signal, or "switching" effect, is observed for both steady state injection and over a range of frequencies modulated in excess of 12 GHz[3]. Initial die devices, developed at Binoptics, posed several difficulties for applications testing: reflections from the access port facets interfered with the injection process; the free-space coupling efficiency was far from optimal; and heating and temperature related effects were not stabilized. The key issues were largely overcome when Infotonics partnered with Binoptics to provide an integrated/packaged version to AFRL for detailed characterization. Metal ferruled lensed fibers with anti-reflection (AR) coatings were incorporated into existing thermo-electric (TE) cooled packages to mitigate the development effort. The multi-port packaging and parallel optimization procedures were reported by Stoffel, et al., in the 2006 Electronic Component Technology Conference submission[4].

Originally we investigated cavity lengths that varied from 400 µm to 1000 µm, but 500 µm was used for the packaged prototypes tested at AFRL. Rather than modulating the drive current (direct modulation), the control over the laser modes was accomplished in this work entirely by optical injection. One of the objectives was to determine if the induced "switching" of mode intensity was primarily due to the stimulating effect of injection, rather than a variation of carrier density, particularly since the former could enable much higher laser response rates.

Enabling Photonics Technologies for Defense, Security, and Aerospace Apps. II,
edited by Michael J. Hayduk, Andrew R. Pirich, Eric J. Donkor, Peter J. Delfyett, Jr.,
Proc. of SPIE Vol. 6243, 62430J, (2006) · 0277-786X/06/$15 · doi: 10.1117/12.670325

It has been shown that increased drive current or a shorter cavity increased the relaxation oscillation frequency. Also an increase in the number of quantum wells in the structure increases the gain which is proportional to the square of the relaxation frequency. Such effects have been thoroughly examined at Binoptics in single cavity Fabry-Perot designs, with relaxation frequencies in excess of 15 GHz being achieved and still higher ones being attainable. The effects of all-optical methods for the modulation, as pursued here, provide an alternative approach. Injected light levels of 2 μW induced switching in prior experiments, but here levels were varied from 100 μW to much higher ones that approached the intensity of the free-running laser so that relaxation effects could be observed in different parameter regimes.

Applications have been proposed in the context of threshold devices in an optical analog to digital conversion[5] or wavelength conversion. Indirect modulators, routers, and optical logic devices are also conceived in digital formats[6,7]. The developments in optically injected Vertical Cavity Surface Emitting Laser (VCSEL) devices have also demonstrated potential in reconfigurable interconnections at high data rates. Such devices share some of the multi-port injection features discussed here, but are based on polarization switching[8] rather than directional propagation[8]. Distinct advantages of the two approaches will become more evident in the course of ongoing work. Certain analog applications may also be considered, since these devices are scaleable and monolithically integrable with optical amplifiers, photodiodes, and electro-absorption modulators (EAMs), etc.

The devices discussed in this work have, to the best of our knowledge, not been previously fabricated or tested. The design having two coupled optical gain paths in a SC medium, with four port interactive optical access, offers unique degrees of freedom for optical control. The large parameter space also presents new challenges to the complex analysis of the device physics. The results presented describe the operating characteristics and phenomenology in the remainder of this paper. A description of the packaged devices and the experimental layout in section 2A is followed by the experimental results for square pulses in section 2B and single frequency inputs in 2C. The injection wavelength detuning effects are discussed in 2D, followed by the theoretical model in section 3 and the discussion and conclusions in section 4.

2. EXPERIMENTAL

2.1 Experimental setup

A prototype packaged ring laser is shown in Figure 1 with an insert photograph of a representative diamond shaped ring laser. The ridge waveguides had width of 3.5 μm with a mode-field size of approximately 3.3 μm that permitted fairly efficient single mode fiber coupling, and the laser output was polarized horizontal to the substrate. A Keithly source delivered the drive current of 80 mA to power the ring laser throughout most of the experiments discussed here. Saturation current (I_{sat}) was ~ 160 mA, while threshold current was ~ 57 mA for the particular module tested. Table 1 describes characteristic parameters, output power (P_{out}) at I_{sat} and return loss (RL), measured for the packaged module.

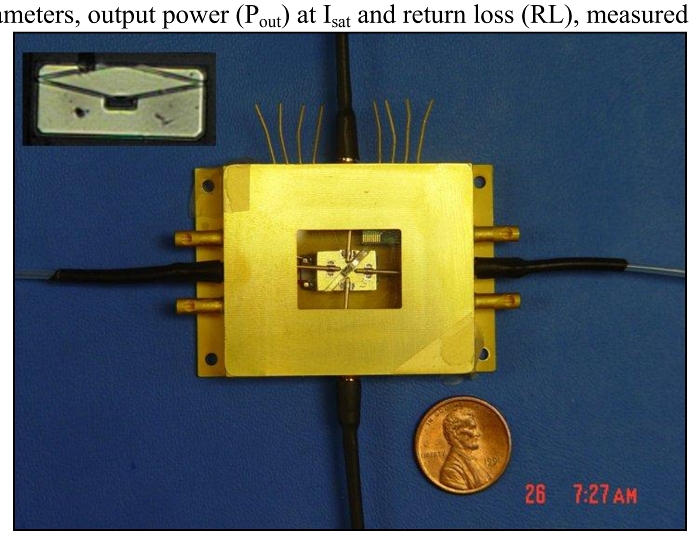

Figure 1. Ring laser package assembled by Infotonics Technology Inc. shown with a photo insert of a diamond shaped ring laser with ~ 500 μm length cavity.

Table 1. Characteristics of Packaged Ring Laser (Module #13)

Fiber Channel	A1	A2	B1	B2
P_{out} at I_{sat}=160 mA	1.49 mW	2.09 mW	2.06 mW	1.70 mW
RL	-23.23 dB	-29.31 dB	-27.8 dB	-27.8 dB

Figure 2 illustrates the experimental setup used to characterize the packaged devices. A New Focus tunable laser, model 6300 Velocity, provided an injected power of approximately 500 μW. An erbium-doped fiber amplifier (EDFA), Pritel Inc. LNHPFA-30, was used to provide higher power levels to the JDSU Mach-Zehnder (MZ) modulator, and a polarization controller set the proper state for the modulator. An Agilent signal generator, model 83650B, delivered the RF sinusoidal signal to the modulator, and a Krohn-Hite Corp. precision DC source, model 523, controlled the modulator bias, which was set to operate on the negative slope of the transfer curve. The output from the modulator was connected to an in-line polarization maintaining (PM) fiber power meter, Eigenlite PM 422, which had a dialable attenuator to vary injected light power with a range of +10 dBm to -20 dBm (10 mW to 10 μW), and Discovery Semiconductor 30S Lab Buddy detectors (3 dB @ 18 GHz) monitored the switching waveforms. An Agilent 86142B optical spectrum analyzer (OSA) captured the ring laser and injection laser spectrum, while an HP 54750A oscilloscope with a 50 GHz module displayed the output waveforms.

The signal generators used to impose the waveforms, or encoding, on the modulator were interchanged between an Anritsu 5 Gb/s, 16 bit pulse pattern generator (PG), model MP 1608A, and an HP 83650B, 20 GHz, sinusoidal frequency generator. The MZ modulator was biased at quadrature in both cases. For the digital patterns, amplification was used to increase the 2 volt signal to near the V_π value of 5 volts, so that a "zero" logic signal corresponded to a modulator minimum output, which was near zero, and a logic level of "one" corresponded to the modulator maximum. Because a broadband amplifier distorted the encoded pulse patterns from the PG in certain parameter ranges, precautions were taken to ensure that the regimes tested were free of distortion.

For the sinusoidal input signals, amplification was not required because input signals less than V_π were sufficient to exhibit the switching effects, and a zero reference level was not essential. The sinusoidal driving signal applied to a MZ modulator yields a sine wave in the small signal regime, or linear region of the MZ transfer curve. When amplifying the applied signal the general form of the transfer curve becomes sin(Asin(ωt)) which is a Bessel function of the first kind. In other words, nonlinear characteristics are manifested gradually with increased signal in the form of higher orders effects, which can be displayed on a spectrum analyzer before there is an effect on the waveform's shape. Amplification was therefore used only to maximize the signal to a level that did not exhibit noticeable distortion of the waveform's shape.

Unless otherwise noted the data resulted from injecting into port A2; the clockwise (CW) mode followed the injected path and corresponded to port B1 output, while the counter-clockwise (CCW) mode corresponded to port B2 output, as depicted in Figure 2.

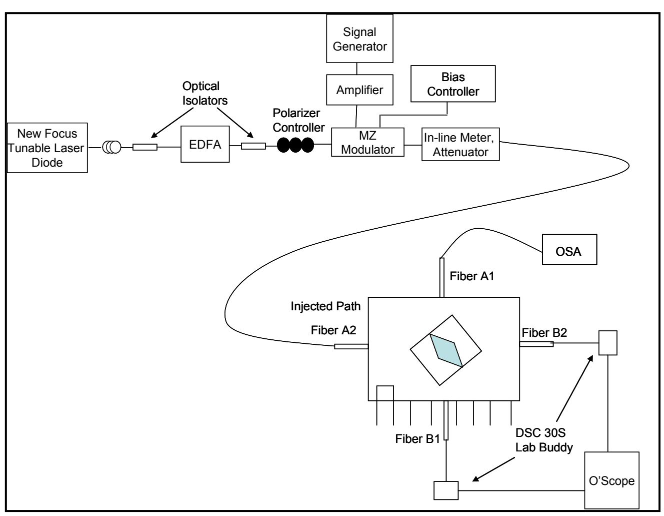

Figure 2. Experimental setup schematic.

2.2 Digital encoded injection

The lowest speed investigated with the pattern generator was 100 Mb/s, with a positive logic bit pattern of 1 on 3 off. Figure 3 shows the positive logic pattern sent from the pattern generator to the MZ modulator, and unless noted the patterns in this paper were positive and either 1 on 3 off or 1 on 1 off.

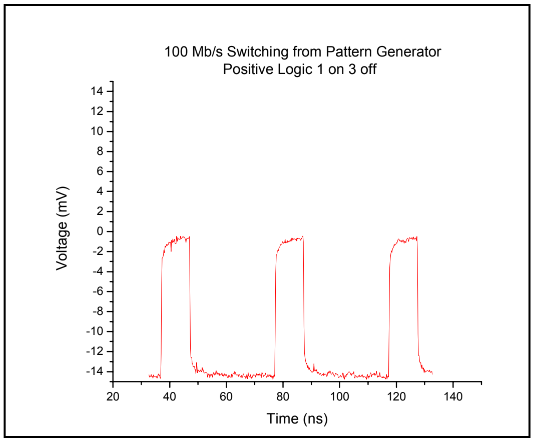

Figure 3. Signal out of the pattern generator imposed on the MZ modulator for 100 Mb/s positive logic pattern 1 on 3 off.

Approximately 1 mW average optical power was injected into the ring laser cavity when it was operating at the higher drive current of 120 mA. The extinction ratio exhibited in Figure 4 can be defined by V_{max}/ V_{min}. The CW mode had larger amplitude because the injected light experienced some gain.

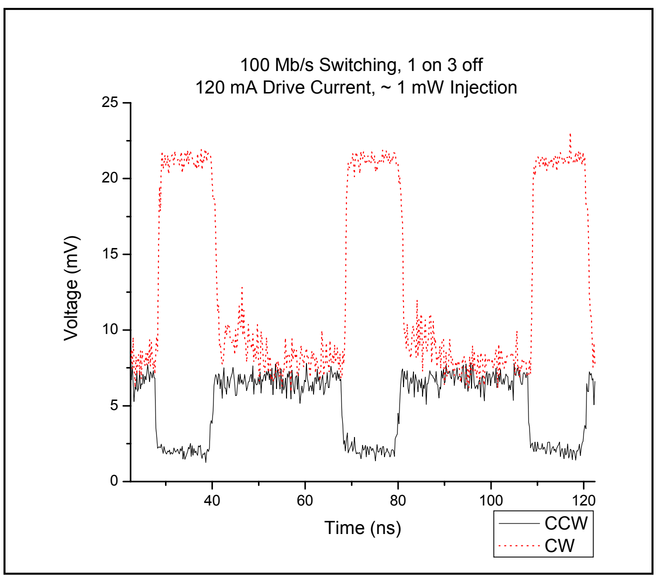

Figure 4. 100 Mb/s switching, bit pattern 1 on 3 off.

Figure 5 shows results for a 1 Gb/s pattern (1 ns injected pulse width), which implies a 250 MHz repetition (rep) rate for the complete 1 on 3 off pattern. Results for both ~ 100 µW and ~ 800 µW average injected optical powers are shown. The extinction ratio for the CCW mode increased from approximately 3 dB to 9 dB with the higher injected power. The structure observed in the output waveforms may be related to relaxation oscillations corresponding to ~ 0.8 GHz, which seems to be independent of injection power if we take the first oscillation peak to be at ~ 25.2 ns for the 800 µW injection case. At higher injection power the oscillations seem to increase in amplitude not frequency.

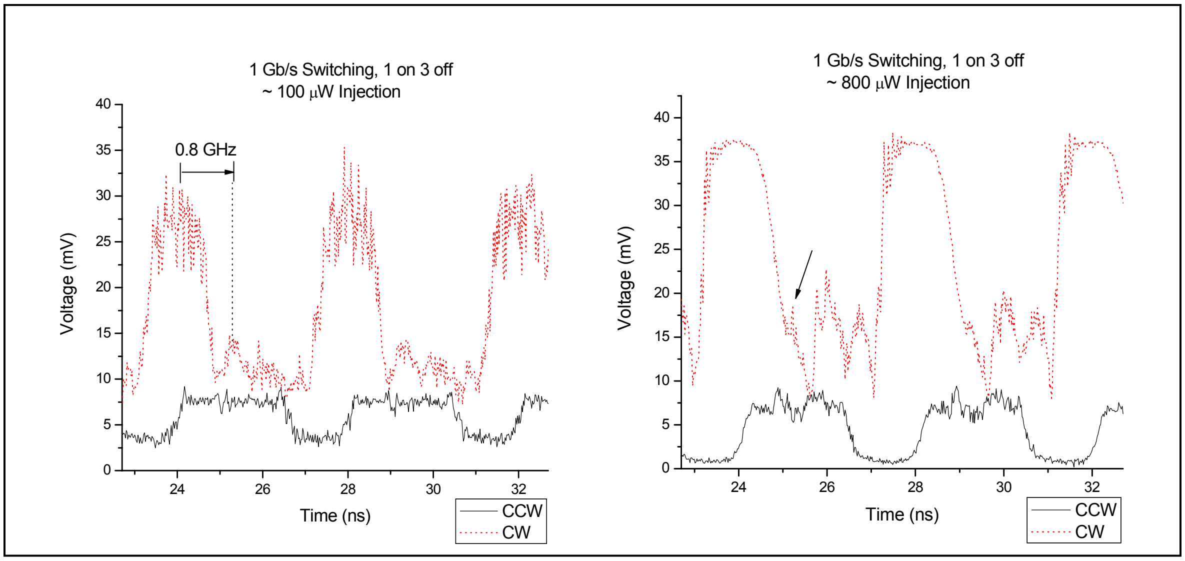

Figure 5. Injection using pattern generator with a 1 Gb/s bit pattern of 1 on 3 off for 100 μW and 800 μW injection.

For comparison purposes, Figure 6 shows that for a sinusoidal 1 GHz injected signal, the oscillations on the waveform correspond to ~ 5 GHz.

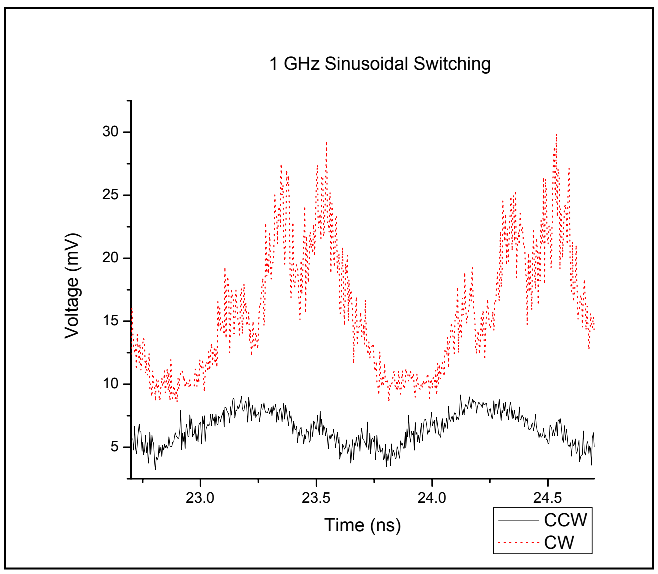

Figure 6. One GHz sinusoidal switching, with ~ 500 μW injected.

Injecting the 4 Gb/s (250 ps pulse) positive logic bit pattern, 1 on 3 off, actually corresponds to a 1 GHz pattern rep rate. Figure 7 depicts that the oscillations, ~ 6 GHz, in this configuration are more prominent than the 1 GHz sinusoidal case and may be related to the high frequency components of the square wave. In both cases the output pulse formation is broadened.

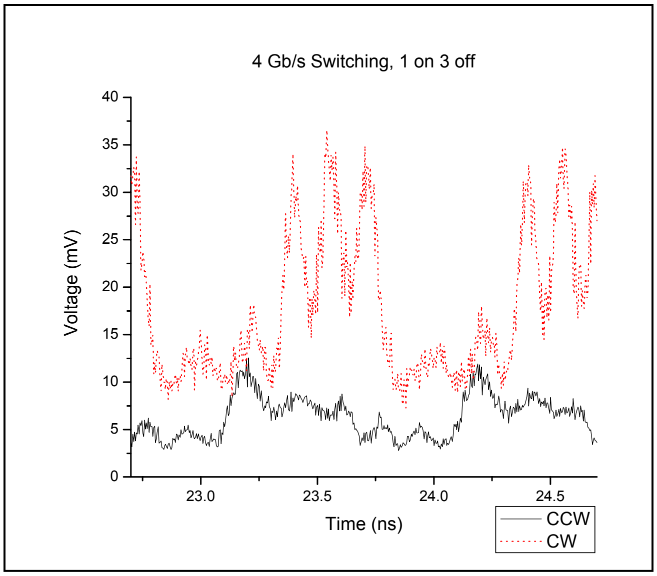

Figure 7. Four Gb/s switching 1 on 3 off corresponds to 1 GHz pattern rep rate, with ~ 500 µW injected.

Figure 8 shows 4 Gb/s negative logic 1 on 3 off, i.e. 1 off 3 on, with a lower optical power injected. This case did not exhibit pulse broadening, but the pulse envelope was not as square shaped as in the positive case. The reason for this difference is not known at this time and cannot be fully explained by the usual rise and fall time responses because of the interaction between the two counter-propagating modes.

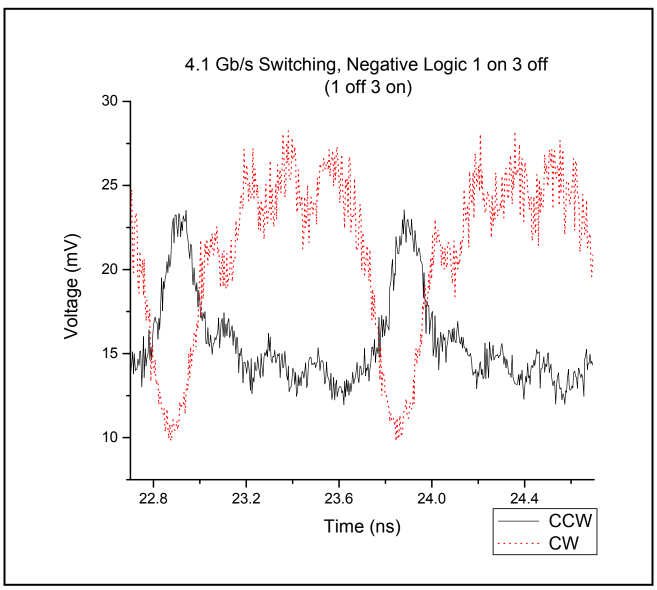

Figure 8. Four GB/s negative logic 1 on 3 off – which is really 1 off 3 on, with ~ 170 µW injected.

For a shorter input pulse, we consider the data in Figure 9 measured by Binoptics on an initial unpackaged device[3] with 600 µm round trip cavity length. The figure shows that for a 100 ps (10 Gb/s) pulse the laser still switched, and the co-propagating trace (bottom right) shows the injected pulse to be reproduced with sufficient fidelity to support selected high speed digital operations. Though the magnitude of the oscillation may have been enhanced by reflections internal to this unpackaged device, the ~ 4 GHz value is in the expected range for such a cavity relaxation oscillation. This was directly supported by observing that increased drive current increased the frequency of the observed oscillation.

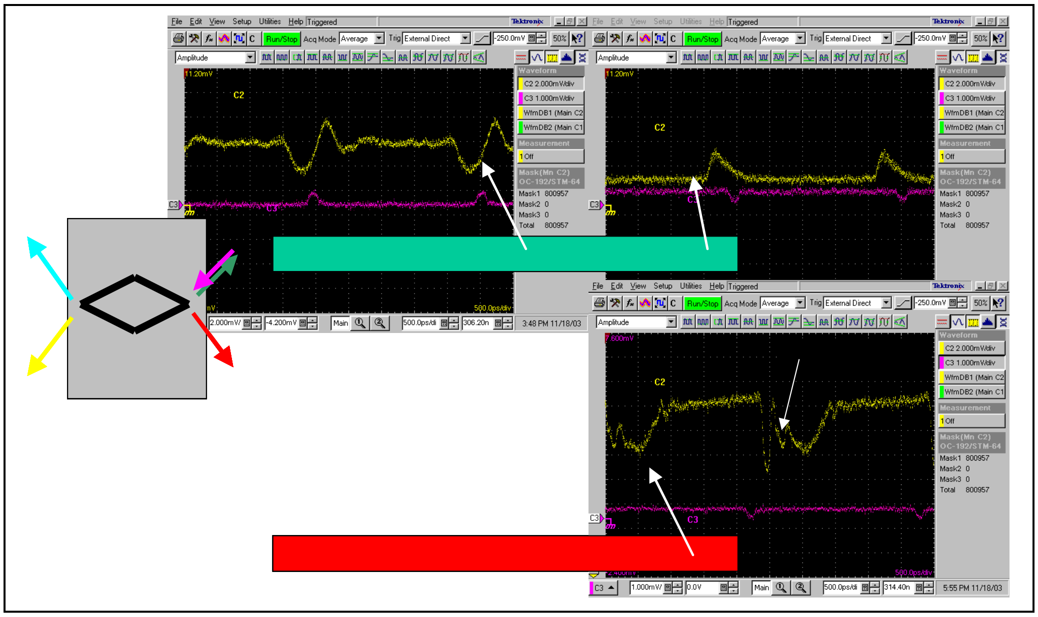
C2
C3

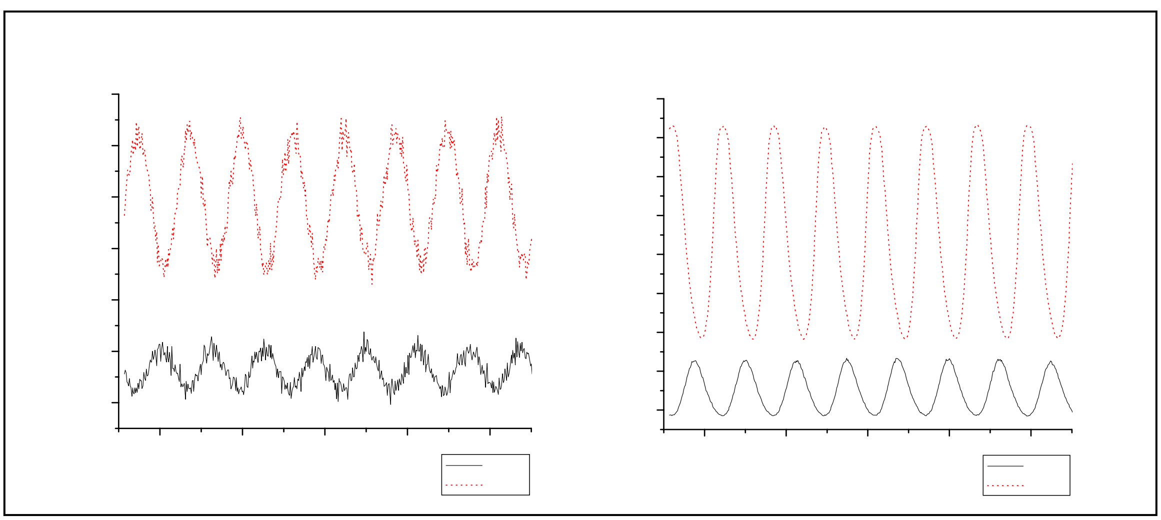

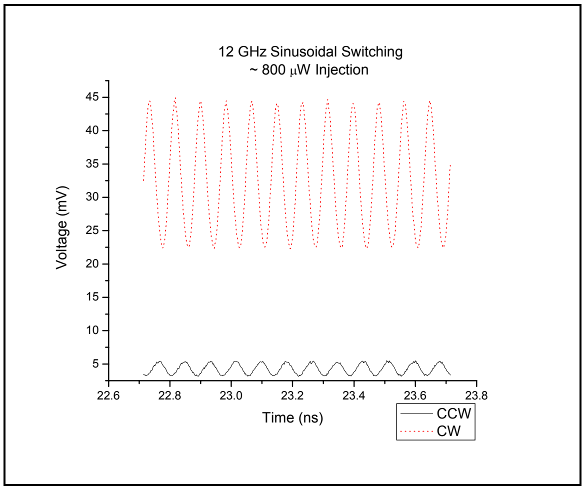

Figure 11. Twelve GHz sinusoidal modulation for 800 µW injection power.

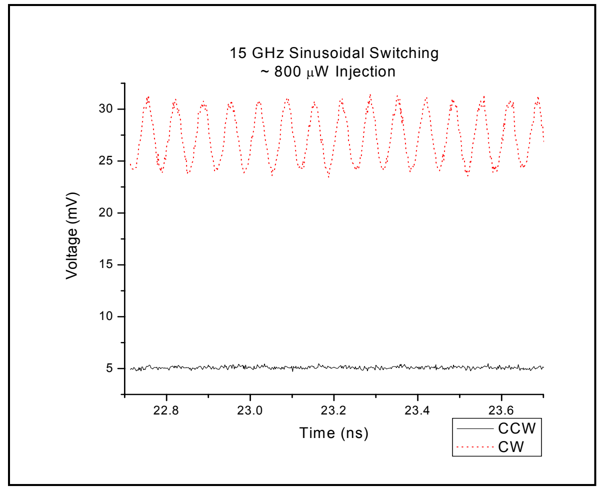

Figure 12. Fifteen GHz sinusoidal modulation shows no response in the CCW mode with 800 µW injected power.

The fiber for port B2 was 200 mm shorter than for port B1, which corresponds to a 1 ns offset between output ports for all of the oscilloscope traces. For our 1 on 3 off patterns this means the 1 Gb/s data set was offset by exactly one (1 ns) pulse bit, whereas for the 4 Gb/s (or other integer) data sets, the offset was exactly one period of the repetition and, therefore, displayed no offset effect. At higher frequencies even a small deviation generated shifts of an appreciable fraction of the period. All of the delays observed in the traces were consistent with the offset described above.

The amplitude of the co-propagating mode was always larger than the CCW direction. This is most likely explained by the limited amount of carriers, so the mode with injection exhibited a dominating effect.

2.4 Detuning of injection wavelength

The injected wavelength was critical to the operation of the SC ring laser switch. When light was injected into the ring laser and aligned with one of the ring cavity modes, the side modes were suppressed to levels approaching 40 dB, depending on the conditions. Figure 12 shows the spectrum of a free running ring laser; there was no spectral effect when the 1 mW of injected light was not aligned to a resonance mode, and the cavity simply acted as a waveguide. Figure 13 also shows the side mode suppression of ~ 34 dB when the injection was aligned within a resonance mode. Alignment did not have to be with the peak mode of the ring laser to force suppression, nor was it necessarily at the exact center of the wavelength overlap.

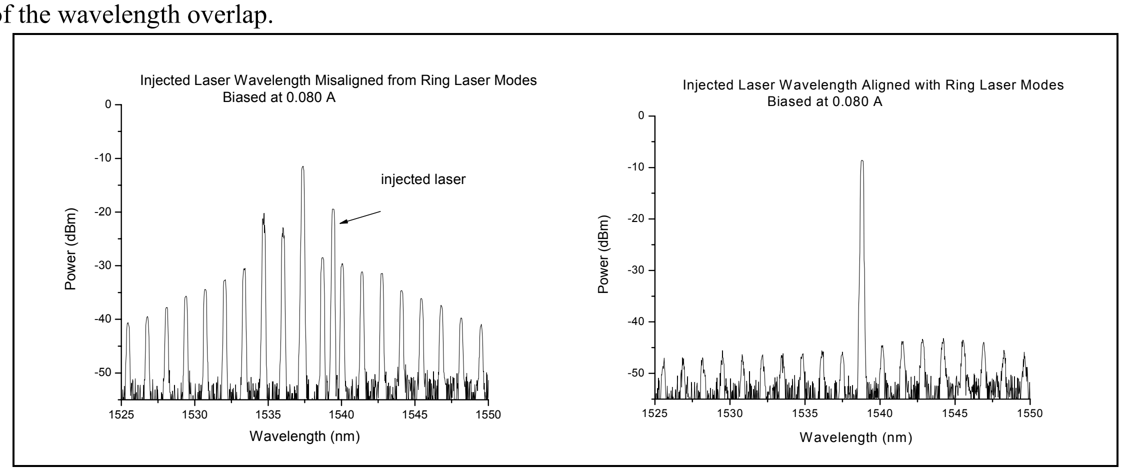

Figure 13. Optical spectrum when the laser injection wavelength was not aligned with ring laser modes and optical spectrum when the laser injection wavelength was aligned with a mode.

The combined injected light and co-propagating mode experienced some gain. In Figure 13 the peak mode amplitude is at - 10 dBm, and after injection was tuned to a mode, it became roughly - 8 dBm.

The wavelength (de)tuning sensitivity was not obvious at lower driving frequencies (f), but at higher frequencies, such as 10 GHz, the RF modulation sidebands imposed on the wavelength center line were resolvable on an OSA. It was observed that optimal switching occurred when the injected wavelength was detuned from the peak of the ring laser by the magnitude of the driving frequency. The frequency offset for optimal switching was also verified at 4 GHz and 1 GHz. At frequencies below 1 GHz, peaks could not be resolved with available equipment. At zero detuning the switching response was extinguished, which can possibly be explained by Figure 18 in the next section.

At such high frequencies the injected wavelength could be detuned by 2f, so the +/- 2nd adjacent sideband became aligned with the center peak of the ring resonance, and with sufficient power injection locking occurred with this second sideband. The effect was two detectable wavelengths propagating in the same direction, which simulated frequency doubling in the output. Figure 14 shows the switching output when the injection was detuned 10 GHz along with the overlaid optical spectrum of the injection and the ring resonance.

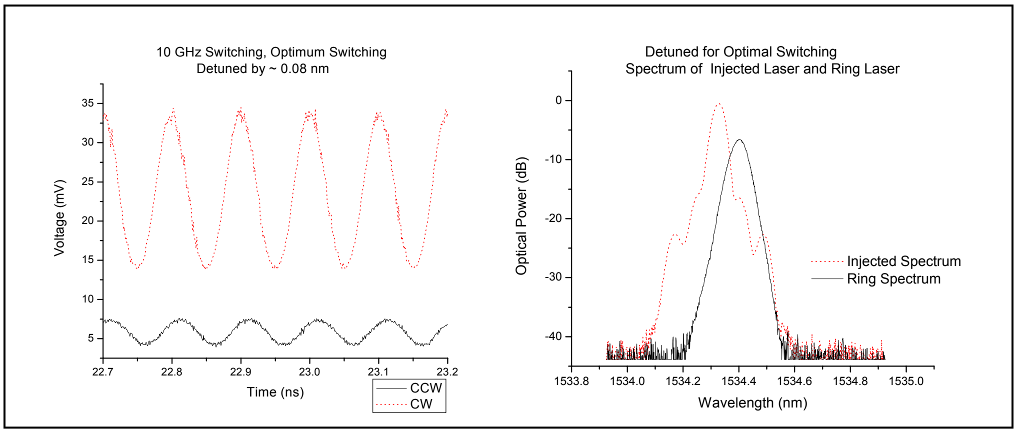

Figure 14. Ten GHz switching with frequency detuned by ~ 10 GHz, and optical spectrum of overlaid injected wavelength and ring laser resonance showing wavelength detuning of ~ 0.08 nm (10 GHz).

Figure 15 illustrates the evolution of the 10 GHz waveform as the wavelength was progressively detuned through the doubling effect. When completely detuned the waveform disappeared indicating complete misalignment and suggesting that the power level available (optical or RF) in the 3rd sideband was not sufficient for inducing the resonant enhancement to drive the switching mechanism.

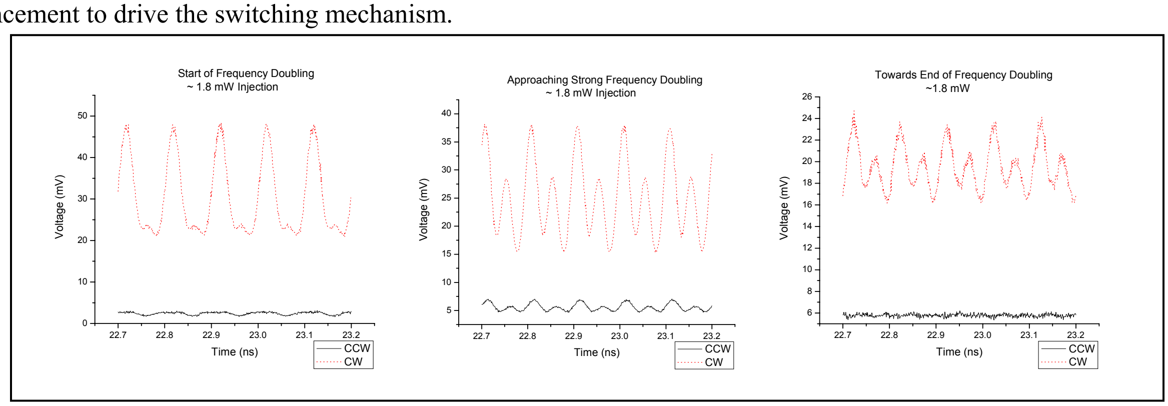

Figure 15. Progression of frequency doubling as an effect of detuning.

3. OPTICAL MODULATION RATE EQUATIONS

In this section we introduce rate equations that model a four port semiconductor ring laser with an optical modulated input signal used for injection locking. Numerical simulations were carried out to illustrate the observed "switching"

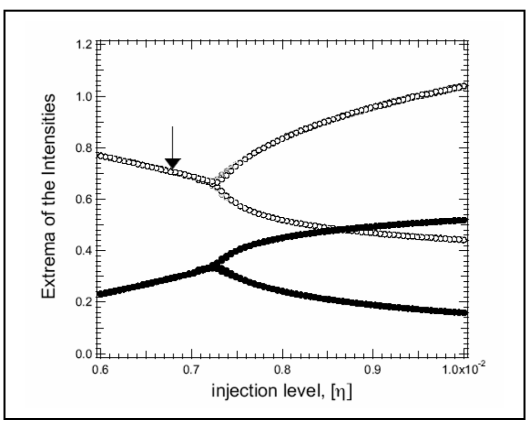

Extrema of the Intensities
injection level, [η]
1.2
1.0
0.8
0.6
0.4
0.2
0.0
0.6
0.7
0.8
0.9
1.0x10^-2

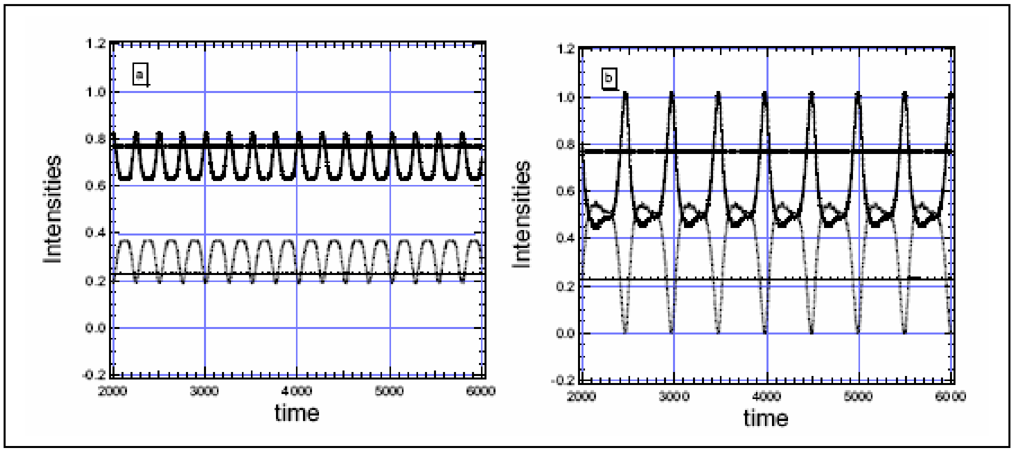

a
b
Intensities
time

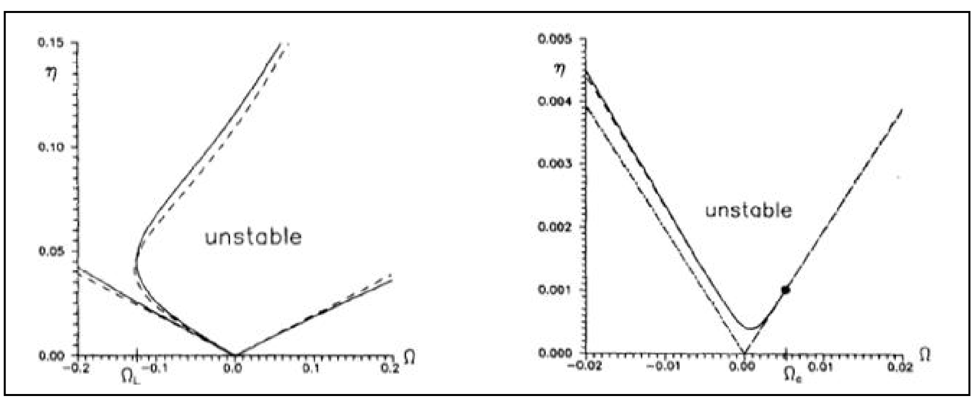

unstable
unstable

4. DISCUSSION AND CONCLUSIONS

The work described here addressed three related questions:

a) For what frequency range can optically induced switching work, and how well?

b) Under which conditions are relaxation effects evident, and to what extent is the potential performance affected?

c) To what degree is the switching effect dependent on carrier density change rather than stimulated photon effects?

Our pulse encoded data yielded some lower frequency effects which may be attributed to residual reflections in the system, but also consistently exhibited oscillations between ~ 4 and 6 GHz, whose behavior was consistent with relaxation effects in the range where they are expected for this medium and cavity dimension. Their effect was not evident for most nearly single frequency input signals, which may be due to their much smaller perturbation to the steady state than a square waveform. No response is expected when the drive current of a diode laser is directly modulated beyond its relaxation frequency, so our observations at up to twice that value with time-varying optical injection may indicate a contribution to switching effects by photon stimulation. However, the observed cutoff at about 15 GHz could imply that the relaxation effects still play a limiting role, and that a combined effect is at work. Conclusions must at this point be guarded until more complete tests are done with sufficient cavity variation to both alter, and isolate, the contribution of the relaxation oscillation. These methods have been successfully demonstrated at Binoptics in Fabry-Perot semiconductor diode lasers, but not in this significantly more complex configuration.

We have characterized a new diamond cavity ring laser design. The unique assembly provided four-port lensed fiber access and ensured stability in the three prototype packages made for testing the devices. Optically switched extinction ratios of ~ 9 dB were observed, but that value could be increased with higher injected power. Optimum switching occurred when the wavelength was detuned, or offset, to match the injected modulation frequency. A theoretical model showed that with proper conditions the laser mode intensities are expected to be anti-correlated with laser injection, as we observed. Further characterization and modeling are being pursued at AFRL/SNDP.

ACKNOWLEDGMENTS

This work was supported through AFRL Grant Award F30602-03-2-0228.

REFERENCES

1. See Binoptics Website:www.binoptics.com
2. Roy Lang, "Injection Locking Properties of a Semiconductor Laser," *IEEE J. of Quantum Electronics,* **18**, No. 6, 976-983, June 1982.
3. Malcolm Green, "Optical Injection and Switching using Diamond Shaped Semiconductor Ring Lasers for Analog to Digital Photonic Converters," *AFRL-SN-RS-TR-2003-308*, Jan. 2004.
4. Nancy Stoffel, Songsheng Tan, Charles Shick, Wesley Bacon, Bryan Beaman, Alan Morrow, Malcolm Green, Rebecca Bussjager, Steve Johns, Michael Hayduk, Joseph Osman, Reinhard Erdmann, and Brian McKeon, "Diamond Shaped Ring Laser Characterization, Package Design and Performance," *ECTC Proceedings*, (to be published 2006).
5. Rebecca Bussjager, Michael J. Hayduk, Steven Johns, Michael Fanto, Reinhard Erdmann, Joseph Osman, and David Winter, *Photonic ADC Final Report Tech Memo*, (to be published 2006).
6. Jürgen Hörer and Erwin Patzak, "Large-Signal Analysis of All-Optical Wavelength Conversion Using Two-Mode Injection-Locking in Semiconductor Lasers," *IEEE J. of Quantum Electronics*, Vol. 33, No. 4, 596-608, Apr. 1997.
7. W. J. Grande and C. L. Tang, "Semiconductor Laser Logic Gate Suitable for Monolithic Integration," *Appl. Phys. Lett.* **51**, No. 22, 1780, Nov. 1987.
8. I. Gatare, M. Sciamanna, J. Buesa, H. Thienpont, and K. Panajotov, "Nonlinear Dynamics Accompanying Polarization Switching in Vertical-Cavity Surface-Emitting Lasers with Orthogonal Optical Injection," *Appl. Phys. Lett.*, **88**, 101106-1 – 101106-3, 2006.
9. P. M. Alsing, V. Kovanis, and A. Gavrielides and T. Erneux, "Lang and Kobayashi Phase Equation," *Physical Review A,* **53**, 4429–4434, 1996.
10. V. Kovanis, A. Gavrielides, T. B. Simpson, and J. M. Liu, "Instabilities and Chaos in Optically Injected Semiconductor Lasers," *Appl. Phys. Lett.*, **67**, 2780-2782, 1995.
11. A. Gavrielides, V. Kovanis, and T. Erneux, "Analytical Stability Boundaries for a Semiconductor Laser Subject to Optical Injection," *Optics Communications*, **136**, 253-256, 1997.